Supplementary material: Self-organising proporties of polar auxin transport

Klaartje van Berkel[1,2], Rob J. de Boer[2], Ben Scheres[1], Kirsten ten Tusscher[2]

[1]Molecular Genetics Group, Department of Biology, Utrecht University, Padualaan 8, 3584 CH Utrecht, The Netherlands

[2]Theoretical Biology Group, Department of Biology, Utrecht University, Padualaan 8, 3584 CH Utrecht, The Netherlands

S.1 Phase plane analysis

To study the dynamic behaviour of the simplified models we use the so-called method of phase plane analysis (figure S.1, table S.1) . This method can be applied if the model consists of two variables (P and A at membrane segment level) or when the model has been further simplified to two variables (P_0 and P_1 at single cell level, when auxin dynamics are assumed to be in quasi steady state). The major idea behind the method of phase plane analysis is to depict the dynamics of the two model variables in a 2-dimensional plane (the phase plane).

Consider a general model with two variables x and y, whose dynamics are typically dependent on each other (e.g. P and A or P_0 and P_1). For this model system we can draw a phase plane with x on the horizontal and y on the vertical axis. Each point in this phase plane represents a potential state of the model system, its coordinates representing the values of x and y in this state. In this phase plane we can depict the dynamics of the variables at each point, using horizontal arrows to depict increases ($\rightarrow$) and decreases ($\leftarrow$) in x and vertical arrows to depict increases ($\uparrow$) and decreases ($\downarrow$) in y. Together these arrows constitute a vector field (note that we can determine the dynamics of x and y in a point simply from the values of $\frac{dx}{dt}$ and $\frac{dy}{dt}$ in that point).

A phase plane contains two (sets of) equilibrium lines, also named isoclines, for which one of the variables does not change in time. These lines are obtained by setting the equation $\frac{dx}{dt}$ or $\frac{dy}{dt}$, respectively, equal to 0. The vector field for each variable switches sign when crossing the respective equilibrium line. Change of this variable is either positive (growth) below or to the left of the equilibrium line and negative (decrease) above or to the right, or *vice versa*. When these equilibrium lines intersect, both variables are in steady state and an equilibrium occurs. Equilibria can be stable (figure S.1**A**) or unstable (figure S.1**B**). When a system that is in a stable equilibrium is perturbed, it will move back to this equilibrium. When the equilibrium is unstable, a perturbation will cause the system to move away from it. Stability of equilibria can often be determined directly by looking at the vector field: if all arrows point towards the equilibrium it is stable, if one or more arrows point away from the equilibrium it is unstable.

A crucial point in our analysis is the distinction between systems with one and systems with multiple stable states. In systems with a single stable equilibrium the system's state will in the long run converge to that equilibrium. In contrast, in bistable system where two stable equilibria are separated by an unstable equilibrium the initial conditions of the system determine to which of the two stable equilibria the system converges (figure S.1**C**).

S.1.1 Difference between single equilibrium and bistable system

Figure S.2 illustrates the differences in behaviour at the single cell level between a system with one stable equilibrium and a bistable system. In the absence of transient perturbations or an external gradient (fig S.2**A** and **D**), the system can be in a symmetric equilibrium in which $P_0 = P_1$. When transiently perturbed from this symmetric

Table S.1: Summary of terms

term	meaning
system	one or more coupled variables for which a differential equation describes the change over time
phase plane (2D)	all possible combinations of x and y values i.e. all possible states of the system
vector field	representation of direction of change for each variable at each position in the phase plane
equilibrium line, isocline	x and y values for which one of the variables does not change
equilibrium	point in which two equilibrium lines intersect and both variables do not change
stable equilibrium, attractor	equilibrium to which a system converges
unstable equilibrium	equilibrium from which a system diverges when perturbed
bistability	situation in which a system has two stable equilibria, separated by an unstable one; or more generally a situation in which a system has an unstable equilibrium separating two distinct long term attractors of the system
PAT model interpretation	
bistability (membrane segment)	a membrane segment either has high or low concentration of PIN proteins
polarity (cell)	a single cell contains at least one membrane segment with high PIN concentration and at least one with low PIN concentration
gradient-driven pattern formation (tissue)	cells within the tissue are not polar, constant sources and sinks keep patterns intact
self-organisation (tissue)	externally applied biases like sources and sinks are not required to maintain a pattern
polarity-driven self-organisation (tissue)	self-organisation results from the ability of single cells to polarise

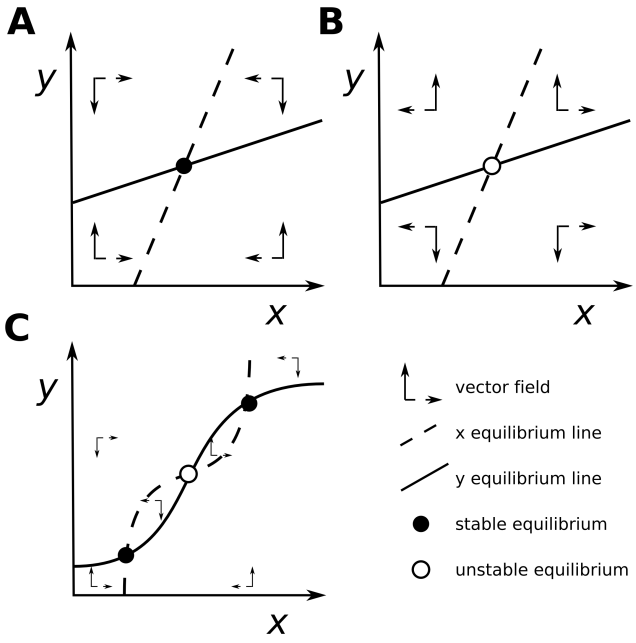

Figure S.1: Examples of phase planes of x and y. Two arbitrary straight equilibrium lines intersect once, providing one equilibrium (**A** and **B**). Depending on the equations (not shown) the vector field can point toward (**A**) or away (**B**) from the equilibrium, i.e. the equilibrium is either stable or unstable. **C**: example of a bistable system. The two equilibrium lines intersect three times. The vector field shows that the outer two equilibria are stable whereas the middle one is unstable.

equilibrium by increasing P_0 (red dots in fig S.2**B** and **E**), the single equilibrium system will eventually return to its symmetrical equilibrium (fig S.2**B**) whereas the bistable system will leave its unstable symmetrical equilibrium and converge to the stable polar equilibrium in which P_0 is high and P_1 is low (fig **S.2E**). Figure **C** shows in red how the phase plane of the single equilibrium model changes when the cell lies in an external auxin gradient. Due to the gradient the membranes of the cells now experience different auxin concentrations, causing P_0 and P_1 to become different from each other such that the single stable equilibrium is no longer symmetrical ($P_0 > P_1$, or *vice versa* in case of the opposite gradient). Figure F shows in red how the phase plane changes for the bistable model when the cell lies in an auxin gradient. We see that the region of the phase plane for which the system will converge to the $P_0 \gg P_1$ polar state (boundary of which is given by the dotted line) becomes larger and now includes the symmetrical initial conditions. Now, even when the cell is initiated in a uniform, symmetrical, state, it will polarise. Note that the polar stable equilibria in fig S.2**D-F** are fundamentally different from the somewhat polarised state in **C**. In the former case, the system is strictly polar, whereas the different concentrations of P_0 and P_1 obtained in the latter are a direct result of the external auxin gradient.

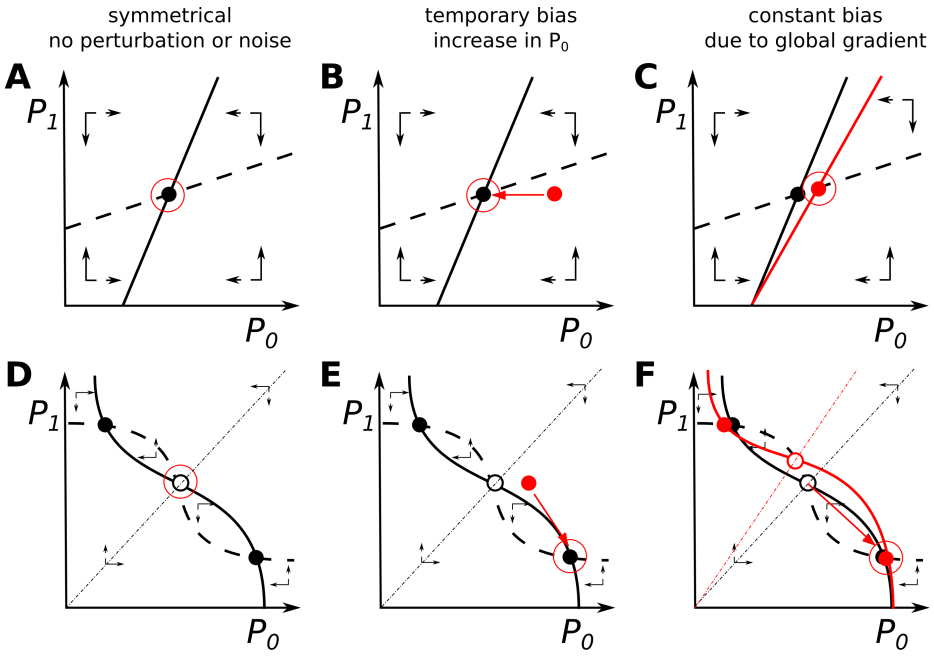

Figure S.2: Phase planes of single equilibrium (**A**-**C**) and bistable (**D**-**F**) single cell models and reactions to temporal perturbations or a global gradient. **A** and **D**: no perturbations or gradient present. **B** and **E**: phase plane after perturbation by increasing the level of P_0. **C** and **F**: change of phase plane when a constant global gradient is present. Solid equilibrium lines are for P_0, dotted equilibrium lines are for P_1. The equilibrium to which a system converges is markes with a large red circle. Red dots in **B** and **E** are initial conditions in which P_0 is slightly increased. In **C** and **F**, altered equilibrium lines and equilibria are marked in red.

S.2 Mathematical framework to study PAT models

S.2.1 Membrane segment model analysis

The caricature membrane segment model consists of an equation for the PIN level at the membrane segment (P) and and equation for auxin in the adjoining neighbouring cell (A). All other PIN and auxin concentrations are assumed to be constant. We use these two variables for all discussed models, but take into account the specific mathematical details of individual models. All phase planes are drawn with P on the y- and A on the x-axis. However, in some cases it is much easier to write A as a function of P.

The default auxin equation is given by:

$$\frac{dA}{dt} = p + i_{pas} + i_{pin}P - eA - dA \tag{S.1}$$

p and d are the production and decay rates respectively. i_{pas} is the passive and $i_{pin}P$ the active rate of influx over the membrane of interest and into the neighbouring cell. Efflux occurs at rate e. A number of models takes into account saturation of auxin transport through the PIN proteins. In our caricature membrane segment model, this translates into:

$$\frac{dA}{dt} = p + i_{pas} + i_{pin}P - (e_{pas} + \frac{e_{pin}}{h_{pin} + A})A - dA \tag{S.2}$$

Note that the $i_{pin}P$ term is not affected, since auxin concentration in the cell to which the membrane segment belongs is assumed to be constant. Instead, we split up the efflux from the neighbouring cell of interest into

a passive (e_{pas}) and active efflux (e_{pin}), the latter of which saturates with the auxin concentration and is half maximum when $A = h$.

The auxin equilibrium line is obtained by setting $\frac{dA}{dt} = 0$. The default auxin equilibrium line is given by (eq 1 in box 1 in the main text):

$$P = \frac{(e+d)A - p - i_{pas}}{i_{pin}} \tag{S.3}$$

If PIN-mediated efflux is saturated, the auxin equilibrium line is given by:

$$P = \frac{(e_{pas} + \frac{e_{pin}}{h_{pin}+A} + d)A - p - i_{pas}}{i_{pin}} \tag{S.4}$$

Ignoring auxin feedback on PIN dynamics for a moment, the equation for PIN dynamics can be written as (eq 3 in box 1 in the main text):

$$\frac{dP}{dt} = k_{on} - k_{off}P \tag{S.5}$$

Depending on the type of feedback of auxin on PIN dynamics, either exocytosis rate k_{on} or endocytosis rate k_{off} depend on auxin flux or concentration.

The assumption of a limiting PIN pool affects PIN dynamics as the membrane segment of interest depletes the pool and thus inhibits its own availability of PINs. This alters the PIN equation to:

$$\frac{dP}{dt} = k_{on}(P_{tot} - P) - k_{off}P \tag{S.6}$$

In which P_{tot} is the total amount of PINs the cell contains. In some models the cytosolic PIN pool is modeled dynamically.

S.2.2 Single cell model analysis

Our single cell model consists of one cell containing PIN levels on two membrane segments (P_0 and P_1) and auxin levels in the two corresponding neighbouring cells (A_0 and A_1). As for the membrane segment model, all other PIN and auxin concentrations are assumed to be constant. Equations for auxin are the same as for the membrane segment model (eq S.1 or S.2) and the same is true for the PIN equation if there is no limiting PIN pool (equation S.5). If there is a PIN pool, it is now depleted by both membrane segments:

$$\frac{dP_i}{dt} = k_{on}(P_{tot} - \sum_n P_i) - k_{off}P_i \quad \text{with } i = 0, 1 \tag{S.7}$$

with n being the total number of membrane segments belonging to one cell. In order to simplify this 4 variable model into a 2 variable model that we can analyse using the phase plane method, we assume that auxin dynamics are fast and hence are in steady state. This allows us to use a so-called quasi steady state (QSS) assumption for auxin dynamics, setting the auxin differential equations to 0. For the simplest auxin equation (eq S.1) we then find:

$$A_i = \frac{p + i_{pas} + i_{pin}P_i}{e+d} \tag{S.8}$$

Substituting equation S.8 in the PIN equations now leaves us with a 2-variable system that we can study with phase plane analysis. Hence, most single cell phase planes will have P_1 on the y- and P_0 on the x-axis. In some cases, however, the authors have already implemented a QSS for the PIN equations and we draw a phase plane for A_1 and A_0 instead.

S.2.3 Concentration, flux and the shape of the PIN equilibrium line

To determine the precise shape of the PIN equilibrium lines in both the membrane segment and single cell models we need to fill in the feedback of auxin on PIN cycling dynamics. Feedback of auxin on membrane PIN levels occurs in most models through either auxin concentrations in neighbouring cells or through auxin fluxes across the membrane.

S.2.3.1 Concentration-based feedback

First let us consider a few elementary shapes for the function describing feedback of auxin concentration on PIN cycling. We use the example of feedback through k_{on}. Feedback on k_{off} will give similar results. A number of ways in which k_{on} might depend on auxin concentration in the neighbouring cell are: linear ($k_{on} = k_{on_b} + k_{on_f} A$), superlinear (e,g, quadratic, $k_{on} = k_{on_b} + k_{on_f} A^2$) or saturating with A ($k_{on} = k_{on_b} + \frac{k_{on_b} A^n}{h_A^n + A^n}$). In all cases, k_{on_b} is the basal exocytosis rate, k_{on_f} is the extra exocytosis rate that depends on auxin. In case of the saturating feedback h_A is the auxin concentration for which k_{on} is half maximum. If $n > 1$, the saturation is sigmoid.

Substituting these into the PIN equation without a limiting PIN pool (eq S.5) and putting it to zero would produce the following PIN equilibrium lines (all phase planes are shown in fig S.3 with a reference to the equation that produces the PIN equilibrium line):

1: linear feedback and unlimiting PIN pool:

$$P = \frac{k_{on_b} + k_{on_f} A}{k_{off}} \tag{Conc.1.a}$$

2: quadratic feedback and unlimiting PIN pool:

$$P = \frac{k_{on_b} + k_{on_f} A^2}{k_{off}} \tag{Conc.2.a}$$

3: saturating feedback and unlimiting PIN pool:

$$P = \frac{k_{on_b}}{k_{off}} + \frac{k_{on_f} A^n}{k_{off}(h_A^n + A^n)} \tag{Conc.3.a}$$

If instead the PIN pool is limiting (eq S.6), the PIN equilibrium lines become:

4: linear feedback and limiting PIN pool:

$$P = \frac{P_{tot}(k_{on_b} + k_{on_f} A)}{k_{off} + k_{on_b} + k_{on_f} A} \tag{Conc.1.b}$$

5: quadratic feedback and limiting PIN pool:

$$P = \frac{P_{tot}(k_{on_b} + k_{on_f} A^2)}{k_{off} + k_{on_b} + k_{on_f} A^2} \tag{Conc.2.b}$$

6: saturating feedback and limiting PIN pool:

$$P = \frac{P_{tot}(k_{on_b} h_A^n + (k_{on_b} + k_{on_f}) A^n)}{((k_{on_b} + k_{off}) h_A^n + (k_{on_b} + k_{on_f} + k_{off}) A^n)} \tag{Conc.3.b}$$

Hence, the addition of a limiting PIN pool effectively alters the linear PIN equilibrium (eq Conc.1.a) line into a line that saturates with auxin (eq Conc.1.b) and the quadratic PIN equilibrium (eq Conc.2.a) line into a sigmoid one (eq Conc.2.b). If the feedback was already saturating, the limiting PIN pool changes the exact position, but not the shape of the PIN equilibrium line (compare eq Conc.3.a and eq Conc.3.b).

S.2.3.2 Flux-based feedback

In order to fill in the feedback of auxin flux on PIN cycling we first need to formulate an expression for across membrane auxin flux, which we will derive here. Both at the membrane segment and single cell level we study PIN concentrations at a membrane segment and the auxin concentration in the corresponding neighbouring cell. Flux is regarded with respect to the membrane segment(s) of interest and is positive in case of net efflux and negative in case of net influx. Hence the equation for (non-saturating) flux (F) is:

$$F = i_{pas} + i_{pin}P - eA \tag{S.9}$$

Note that we use the same nomenclature as for the auxin in the neighbouring cell (i_{pas} and i_{PIN} are influxes into the neighbouring cell and effluxes over the membrane segment of interest, e is efflux from the neighbouring cell and influx over the membrane segment of interest). Similarly, since the focus is on the membrane segment (with PIN level P) and its neighbouring cell (with auxin level A), the auxin in the cell to which the membrane segment belongs is assumed to be constant, and is incorporated in i_{pas} and i_{pin}. Most flux-based models assume that only net efflux feeds back on PIN localisation, using a Heaviside function $\theta(F)$ to switch feedback on if flux is positive and off if flux is negative.

Now let us consider the same elementary shapes for flux feedback functions and the PIN equilibrium lines they produce. It is important to notice that when calculating the flux, both P and A are taken into account. Hence, if flux feeds back on PIN cycling, the PIN concentration feeds back on itself.

1: linear feedback ($k_{on} = k_{on_b} + k_{on_f}\theta(F)F$) and unlimiting PIN pool:

$$P = \begin{cases} \frac{k_{on_b}}{k_{off}} & \text{if } F \leq 0 \\ \frac{k_{on_f}(eA - i_{pas}) - k_{on_b}}{k_{on_f} i_{pin} - k_{off}} & \text{if } F > 0 \end{cases} \tag{Flux.1.a}$$

2: quadratic feedback ($k_{on} = k_{on_b} + k_{on_f}\theta(F)F^2$) and unlimiting PIN pool:

$$P = \begin{cases} \frac{k_{on_b}}{k_{off}} & \text{if } F \leq 0 \\ \frac{2k_{on_f} i_{pin}(eA - i_{pas}) + k_{off} + \sqrt{4k_{on_f} k_{off} i_{pin}(eA - i_{pas}) + k_{off}^2 - 4k_{on_f} i_{pin}^2 k_{on_b}}}{2k_{on_f} i_{pin}^2} & \text{if } F > 0 \end{cases} \tag{Flux.2.a}$$

3: saturating feedback ($k_{on} = k_{on_b} + k_{on_f}\theta(F)\frac{F^n}{h_F^n + F^n}$) and unlimiting PIN pool:

$$\begin{cases} P = \frac{k_{on_b}}{k_{off}} & \text{if } F \leq 0 \\ A = \frac{1}{e}\left(i_{pas} + i_{pin}P + \sqrt[n]{\frac{h_F^n (k_{off}P - k_{on_b})}{k_{off}P - k_{on_b} - k_{on_f}}} \right) & \text{if } F > 0 \end{cases} \tag{Flux.3.a}$$

And, as well, with limiting PIN pool:

4: linear feedback and limiting PIN pool:

$$\begin{cases} P = \frac{k_{on_b} P_{tot}}{k_{off} + k_{on_b}} & \text{if } F \leq 0 \\ A = \frac{k_{on_f}(i_{pas}P + i_{pin}P^2 - i_{pin}P_{tot}P - i_{pas}P_{tot}) - k_{on_b}(P_{tot} - P) + k_{off}P}{k_{on_f} e (P - P_{tot})} & \text{if } F > 0 \end{cases} \tag{Flux.1.b}$$

5: quadratic feedback and limiting PIN pool:

$$\begin{cases} P = \frac{k_{on_b} P_{tot}}{k_{off} + k_{on_b}} & \text{if } F \leq 0 \\ A = \frac{k_{on_f}((i_{pas} + i_{pin}P)(P - P_{tot}) + \sqrt{-k_{on_f}((P - P_{tot})(k_{on_b}P + k_{off}P - k_{on_b}P_{tot}))}}{k_{on_f}(P - P_{tot})e} & \text{if } F > 0 \end{cases} \tag{Flux.2.b}$$

6: saturating feedback and limiting PIN pool:

$$\begin{cases} P = \frac{k_{on_b} P_{tot}}{k_{off} + k_{on_b}} & \text{if } F \leq 0 \\ A = \frac{1}{e}\left(i_{pas} + i_{pin}P - \sqrt[n]{\frac{h_F^n (k_{on_b}P + k_{off}P - k_{on_b}P_{tot})}{k_{on_b}(P_{tot} - P) + k_{on_f}(P_{tot} - P) - k_{off}P}} \right) & \text{if } F > 0 \end{cases} \tag{Flux.3.b}$$

In all cases, the Heaviside function $\theta(F)$ causes a sharp switch in the PIN equilibrium line, which makes it inherently non-linear. The limiting PIN pool causes the PIN equilibrium line to curve back, such that it becomes a sigmoid-like line.

S.3 Membrane segment variants

Here we present an overview of distinct model behaviours at the membrane segment level for all possible combinations of auxin and PIN dynamics. At the membrane segment we can distinguish between systems with one, two (semi-bistable) or three (bistable) equilibria. Different combinations of auxin and PIN equilibrium lines can lead to one of these cases:

MS.I: straight A equilibrium line and (sub)linear P equilibrium line: one equilibrium If the straight A equilibrium line that results from our default auxin equation S.1 is combined with a PIN equilibrium line that is linear or saturates with $n = 1$ (eq Conc.1.a, Conc.1.b, Conc.3.a and Conc.3.b), there can be only one stable equilibrium, and thus no bistability (fig S.3**A**) independent of whether or not a limiting PIN pool is assumed.

MS.II: straight A equilibrium line and superlinear P equilibrium line: two equilibria When the auxin equilibrium line is a straight line (eq S.3 as follows from the auxin eq S.1), bistability can occur when the PIN equilibrium line is superlinear and non-saturating (eq Conc.2.a, Flux.1.a and Flux.2.a). There are two equilibria. The lower equilibrium is stable and the upper unstable. Above the upper equilibrium there is a region of unlimited increase of PIN levels. This situation results in a bistable system, since it has two regions of distinctly different behaviour, even though there is only one stable equilibrium (fig S.3**B**) and an unlimiting PIN pool is assumed.

MS.III: straight A equilibrium line and sigmoid P equilibrium line: three equilibria A straight auxin equilibrium line can intersect thrice with a sigmoid PIN equilibrium line (eq Conc.3.a with $n = 2$, **Conc.2.b**, **Conc.3.b** with $n = 2$, **Flux.1.b**, **Flux.2.b**, **Flux.3.a** and **Flux.3.b**) (fig S.3**C**). The outer two equilibria are stable and the middle one is unstable. Hence, bistability arises from a sigmoid saturating feedback or a non-linear feedback combined with a limiting PIN pool.

MS.IV: both A and P equilibrium lines are non-linear: two or three equilibria Non-linearity in the auxin equilibrium line (eq S.4) can introduce bistability when combined with a PIN equilibrium line that previously would not give bistability (eq **Conc.3.a** with $n = 1$, **Conc.1.b**, **Conc.3.b** with $n = 1$) (fig S.3**D**).

S.4 Single cell variants

At the cell level we are interested in whether the system can display polar behaviour. For this the model needs to have two stable polar equilibria, one with high PIN levels on one membrane segment and low PIN levels on the other and one *vice versa*. The different possible combinations of model assumptions produce a total of three different scenarios, for two of which cell polarity can occur.

SC.I: non-bistable membrane segments combined with a limiting PIN pool: no polarity As an example of this scenario, consider the concentration-based, linear, feedback that is not able to give membrane bistability. Combining this feedback with a limiting PIN pool gives the following PIN equations for P_0 and P_1:

$$\frac{dP_i}{dt} = (k_{on_b} + k_{on_f} A_i)(P_{tot} - P_i - P_j) - k_{off} P_i \quad \text{with } i = 0, 1 \text{ and } j = 1, 0 \tag{S.10}$$

Substituting the auxin QSS, to reduce the system to two variables gives us the full PIN equation:

$$\frac{dP_i}{dt} = \left(k_{on_b} + k_{on_f} \left(\frac{p + i_{pas} + i_{pin} P_i}{e + d}\right)\right)(P_{tot} - P_i - P_j) - k_{off} P_i \quad \text{with } i = 0, 1 \text{ and } j = 1, 0 \tag{S.11}$$

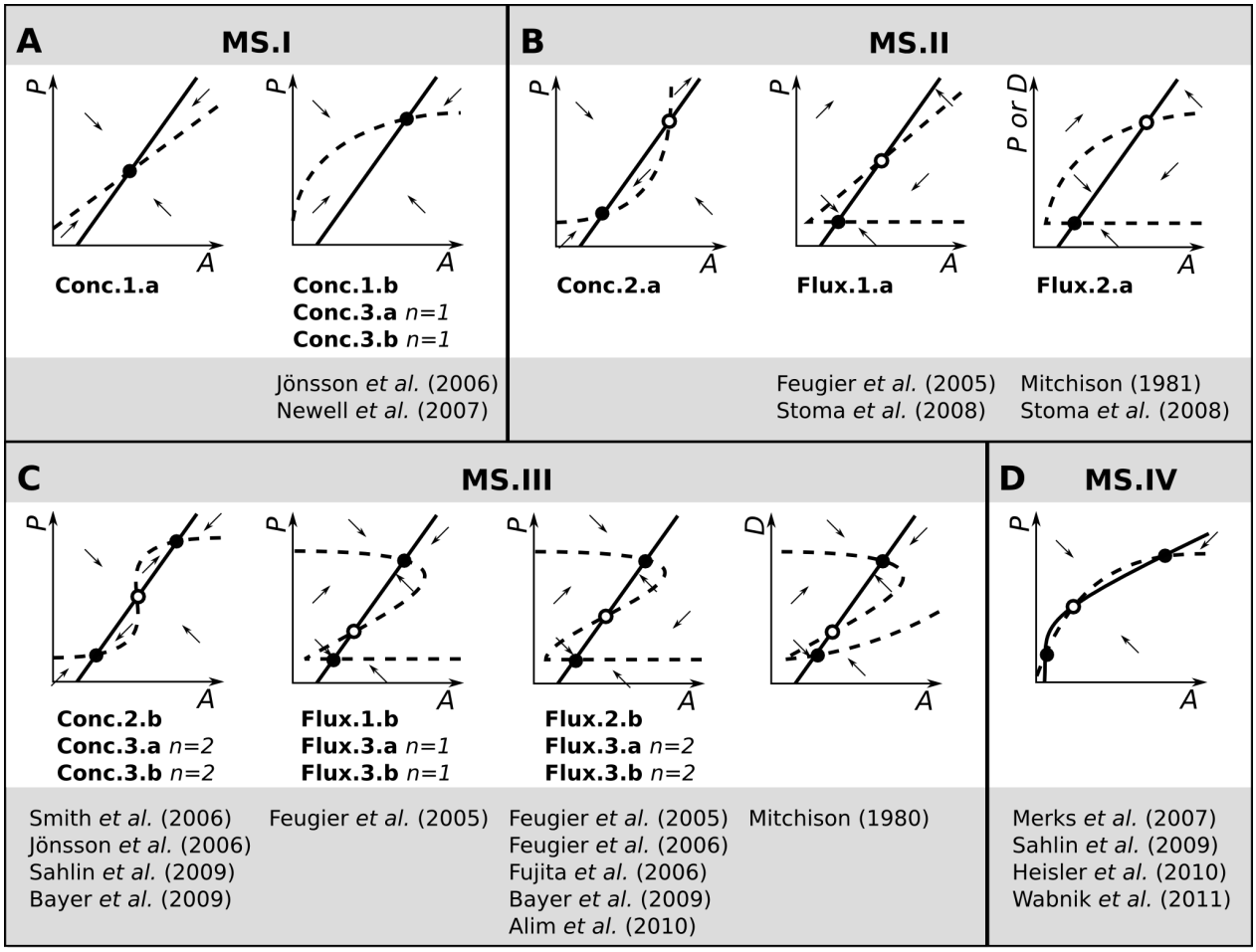

Figure S.3: Overview of the different membrane segment variants with corresponding PIN equilibrium lines and references to PAT models with (similar) auxin and PIN dynamics. Dashed lines: P equilibrium lines. Solid lines: A equilibrium lines. Closed circles: unstable equilibria. Open circles: stable equilibria. Arrows represent the direction of dynamics.

The resulting equilibrium lines are shown in fig S.4**A** Although P_0 and P_1 are interdependent, their equilibrium lines are only able to intersect once in a stable equilibrium in which (given no external bias) $P_0 = P_1$. Hence, no cell polarity occurs.

SC.II: bistability at the membrane segment level combined with a limiting PIN pool: polarity (+ rest state) As an example of this scenario, consider the concentration-based, quadratic, feedback as in equation Conc.2.b. Implementing this feedback at the single cell level gives us the following PIN equations for P_0 and P_1:

$$\frac{dP_i}{dt} = (k_{on_b} + k_{on_f} A_i^2)(P_{tot} - P_i - P_j) - k_{off} P_i \quad \text{with } i = 0,1 \text{ and } j = 1,0 \tag{S.12}$$

Substituting the auxin QSS gives us the full PIN equation:

$$\frac{dP_i}{dt} = \left(k_{on_b} + k_{on_f} \left(\frac{p + i_{pas} + i_{pin} P_i}{e + d}\right)^2\right)(P_{tot} - P_i - P_j) - k_{off} P_i \quad \text{with } i = 0,1 \text{ and } j = 1,0 \tag{S.13}$$

The resulting equilibrium lines can intersect three times (fig S.4**B**). Two of these equilibria are stable and asymmetrical ($P_0 > P_1$ and $P_0 < P_1$), one is unstable and symmetrical ($P_0 \sim P_1$). If a model contains only these three equilibria it polarises automatically due to noise.

Additionally, a third stable equilibrium, and corresponding unstable equilibria, might occur. This happens in case feedback is concentration-based and sigmoid (eq **Conc.3.b** with $n = 2$) and in case of flux-based feedback (due to the Heaviside function). This third equilibrium occurs for $P_0 = P_1$ and represents an apolar rest state. The system has to be sufficiently perturbed from this state in order to become polar.

SC.III: non-bistable membrane segments combined with an unlimiting PIN pool: no polarity As an example, if the linear concentration-based feedback (eq **Conc.1.a**) is combined with an unlimiting PIN pool, the PIN equations become:

$$\frac{dP_i}{dt} = k_{on_b} + k_{on_f} A_i - k_{off} P_i \quad \text{with } i = 0,1 \tag{S.14}$$

Implementing the QSS for A_i gives us the full PIN equations:

$$\frac{dP_i}{dt} = k_{on_b} + k_{on_f} \left(\frac{p + i_{pas} + i_{pin} P_i}{e + d}\right) - k_{off} P_i \quad \text{with } i = 0,1 \tag{S.15}$$

And the resulting PIN equilibrium line:

$$P_i = \frac{k_{on_b}(e + d) + k_{on_f}(p + i_{pas})}{k_{off}(e + d) - k_{on_f} i_{pin}} \quad \text{with } i = 0,1 \tag{S.16}$$

Since this equilibrium line is a mere combination of parameters, it is an exactly horizontal or vertical line in the phase plane. The two equilibrium lines can, thus, only intersect once (fig S.4**C**). The intersection point is a stable equilibrium in which (given no external bias) $P_0 = P_1$. Hence, no cell polarity occurs.

SC.IV: bistability at the membrane segment level combined with an unlimiting PIN pool: polarity (+ rest state + bipolar state) As an example of this scenario, consider the sigmoid concentration-based feedback (**Conc.III.a** with $n = 2$) with an unlimiting PIN pool. The resulting single cell level PIN equation is:

$$\frac{dP_i}{dt} = k_{on_b} + \frac{k_{on_f} A_i^2}{h_A^2 + A_i^2} - k_{off} P_i \quad \text{with } i = 0,1 \tag{S.17}$$

Implementing the QSS for A_i and setting $\frac{dP_i}{dt}$ to 0 gives us three solutions for P_i, i.e. the PIN equilibrium lines are either three horizontal or three vertical lines. These lines intersect a total of nine times, giving rise to five unstable and four stable equilibria (fig S.4**D**). Two of the stable equilibria are polar, one represents the apolar rest state in which $P_0 = P_1$ and both are low, and the last represents a bipolar state in which $P_0 = P_1$ and both are high.

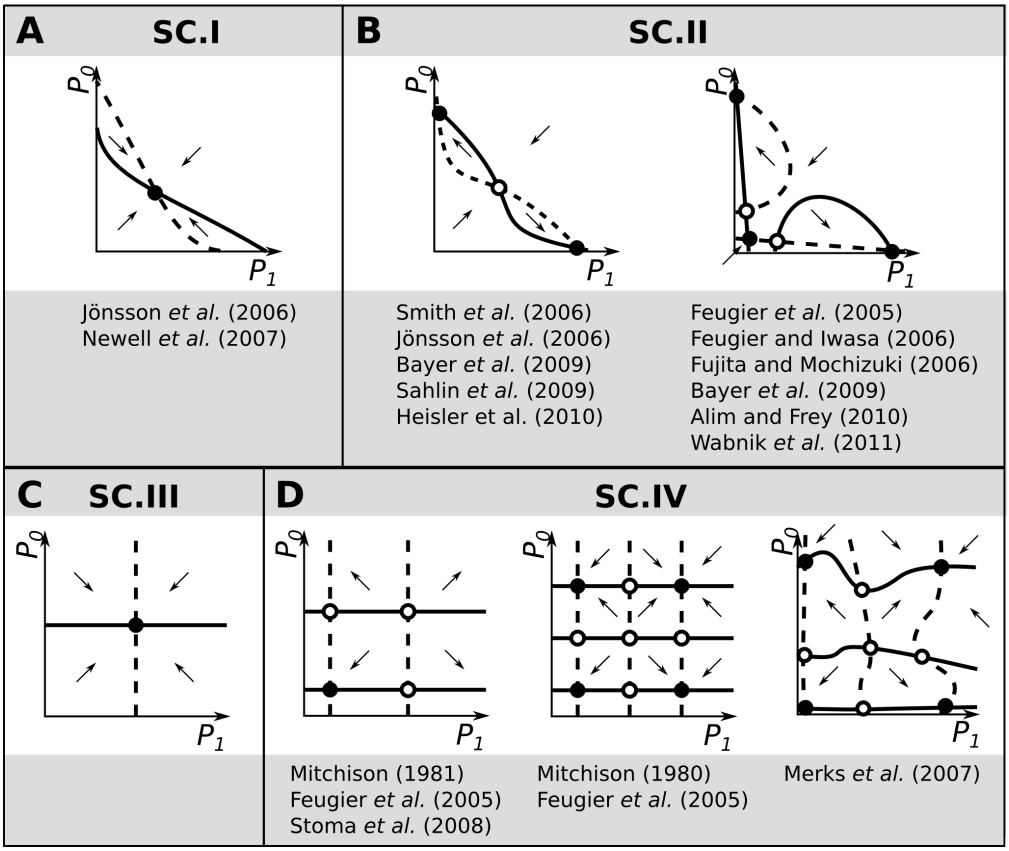

Figure S.4: Overview of the different single cell variants with references to PAT models with (similar) single cell dynamics. Solid lines: P_0 equilibrium lines. Dashed lines: P_1 equilibrium lines. Closed circles: unstable equilibria. Open circles: stable equilibria. Arrows represent the direction of dynamics.

S.5 Analysis of discussed PAT models

Here we describe how we formulated equations for PIN and auxin dynamics at the membrane segment and single cell behaviour and thus analysed model behaviour for the models discussed less extensively in the main text.

S.5.1 Flux based models

S.5.1.1 Mitchison (1980)

Mitchison [1980] developed a model in which membrane segment permeability depends on flux over that membrane. Since his model does not contain PINs, we cannot use our default auxin equation. Translating his model to our membrane segment model gives the following equation for auxin in the neighbouring cell (named "signal" in the original paper):

$$\frac{dA}{dt} = p - dA + F \tag{S.18}$$

in which p is production of the signal. In the original model, signal decay only takes place in a certain area of the tissue. In order to analyse behaviour at the membrane segment and cellular level we replace this with a decay taking place in each cell. Flux depends on the permeability of the membrane segment (D) and consists of the influx over the membrane segment of interest and efflux out of the neighbouring cell

$$F = D - eA \tag{S.19}$$

Together equation S.18 and S.19 give the auxin equilibrium line:

$$A = \frac{p + D}{e + d} \tag{S.20}$$

In turn, membrane permeability, depends on flux in a superlinear, saturating manner (membrane segment variant 1a):

$$D = \alpha \frac{F^2}{\gamma + F^2} + \beta \tag{S.21}$$

Substituting equation S.19 for F and rewriting such that A becomes a function of D gives a quadratic function. Hence, the permeability equilibrium line has two solutions:

$$A = \begin{cases} \frac{\alpha D + \beta D - D^2 + \sqrt{\alpha\gamma D - \alpha\beta\gamma - \gamma D^2 + 2\beta\gamma D - \gamma\beta^2}}{(\alpha - D + \beta)e} & \text{if } F > 0 \\ -\frac{-\alpha D - \beta D + D^2 + \sqrt{\alpha\gamma D - \alpha\beta\gamma - \gamma D^2 + 2\beta\gamma D - \gamma\beta^2}}{(\alpha - D + \beta)e} & \text{if } F \leq 0 \end{cases} \tag{S.22}$$

These two equilibrium lines (equation S.20 and S.22) can intersect in three equilibria, two of which are stable (fig S.3**C**). Hence, bistability can occur at the membrane segment level (**MS.III**).

Each membrane segment in the model determines its permeability without taking into account the other membrane segments of this cell, i.e. there is no competition for a "permeability factor" (**SC.IV**). As a result, there are 9 possible equilibria, 4 of which are stable (fig S.4**D**). Two stable equilibria are symmetrical, they represent apolar cells in which both membrane segments have a low or a high permeability. The two asymmetrical equilibria represent polar cells with a low permeability of one membrane segment and a high permeability of the other.

S.5.1.2 Mitchison (1981)

In his second model [Mitchison, 1981], Mitchison did not take into account production of auxin in individual cells, but instead allowed it to come in from a local source and redistribute along a tissue. On a similar note as above, we replaced this localised production and decay by production and decay processes taking place in each cell. The

auxin equation and auxin equilibrium line therefore remains the same with respect to the previous model (equation S.18 and S.20 respectively).

In this second model, two aspects have changed with respect to the previous model. First, direction of flux is now important. Instead of absolute flux, net efflux feeds back on D. Second, the feedback no longer saturates, but is a quadratic function. In addition, D is now a dynamic variable:

$$\frac{dD}{dt} = \alpha\theta(F)F^2 + \beta - D \tag{S.23}$$

which is equivalent to eq Flux.2.a.β is the basal flux rate over the membrane segment of interest when $F < 0$. By taking into account "degradation" of the permeability ($-D$), Mitchison already hints toward the existence of a physical pump that is subject to turnover.

D now depends as follows on flux:

$$D = \alpha\theta(F)F^2 + \beta \tag{S.24}$$

Substituting the flux and rewriting A as a function of D gives the full D equilibrium line (similar to eq Flux.2.a):

$$\begin{cases} A = \frac{\alpha D + \sqrt{-\alpha\beta + \alpha D}}{\alpha e} & \text{if } F > 0 \\ D = \beta & \text{if } F \leq 0 \end{cases} \tag{S.25}$$

which can intersect twice with the auxin equilibrium line (fig S.3**B**). The bottom equilibrium is stable, the upper equilibrium is unstable. Above this unstable equilbrium, unlimited growth of membrane permeability takes place. Thus bistability can occur at the membrane segment level (**MS.II**).

Similarly to the previous model by the same author, there is no communication between membrane segments of one cell. Therefore the model falls into variant **SC.IV** (fig S.4**D**).

S.5.1.3 Feugier *et al.* (2005)

In Feugier et al. [2005], production of auxin depends on a dynamically modeled enzyme (S):

$$\frac{dS}{dt} = p(1 - \frac{A}{A_{eq}}) - \delta S \tag{S.26}$$

In which p is production of the enzyme, A_{eq} is the value of auxin for which the enzyme production becomes 0 and δ is decay of the enzyme. Setting $\frac{dS}{dt} = 0$ and filling it in in the auxin equation gives:

$$\frac{dA}{dt} = \epsilon\frac{p}{\delta}(1 - \frac{A}{A_{eq}}) + i_{pas} + i_{pin}P - eA \tag{S.27}$$

which gives the same auxin equilibrium line as our default auxin equation (eq S.3). The authors also test the effect of saturated efflux, which does not alter the model's self-organising potential in our analysis.

In this model, net efflux feeds back on k_{on}in 9 different manners, most of which fit into our overview of possible feedback functions (section S.2.3.2). In fig S.3 we indicate which possible combinations of auxin and PIN dynamics are studied in the Feugier et al. [2005] model. All of these give bistable membrane segments (variants **MS.II** and **MS.III**).

When these feedbacks are combined with a limiting PIN pool, they fall into category **SC.II**. If, instead, the PIN pool is unlimiting, the models behave like the **SC.IV** variant.

S.5.1.4 Feugier and Iwasa (2006)

In Feugier and Iwasa [2006], a similar model was used as in the previous paper by the same authors, although slight changes were implemented. The auxin dynamics are described by equation S.1 and thus give the auxin equilibrium line from equation S.3. Net efflux feeds back on k_{on} in a quadratic manner and an limiting PIN pool is assumed. Hence the PIN equation becomes (similar to eq Flux.2.b):

$$\frac{dP}{dt} = (k_{on_b} + k_{on_f}\theta(F)F^2)(P_{tot} - P) - k_{off}P \tag{S.28}$$

With k_{on_b} the basal exocytosis and k_{on_f} the flux-dependent exocytosis. The resulting PIN equilibrium line is given by eq Flux.2.b. Thus, the model behaves as variant **MS.III** (fig S.3**C**). As a result of the superlinear feedback function and the limiting PIN pool, the single cell level is polar (variant **SC.II**, fig S.4**B**).

In this second model, the authors add a "flux-bifurcator" in order to generate loop formation in veins. The additional effects of the flux-bifurcator on the 2-dimensional model behaviour are beyond the scope of our analysis.

S.5.1.5 Fujita and Mochizuki (2006)

Fujita and Mochizuki [2006] studied the stability of a simplified flux-based model. The auxin equation is given by equation S.1 and, thus, the auxin equilibrium line by equation S.3. In the model, flux feeds back on PIN localisation in a superlinear manner. The model is not mechanistic, in that the feedback of flux on PINs is not specific for certain cycling rates. The PIN equation is:

$$\frac{dP_0}{dt} = m\left(\frac{1}{1+\mathrm{e}^{-\alpha(F_0-\beta)}} + \frac{1}{P_{tot}}\left(\frac{1}{1+\mathrm{e}^{-\alpha(F_0-\beta)}} + \frac{1}{1+\mathrm{e}^{-\alpha(F_1-\beta)}}\right)P_0\right) \tag{S.29}$$

In which m is the growth rate, F_0 and F_1 are fluxes over the two membrane segments of one cell (given by equation S.9), respectively, and α and β are constants determining the shape of the feedback. The resulting PIN equilibrium line is given by (which for reasons of simplicity we write for A as a function of P) (similar to eq Flux.3.b):

$$A = \frac{1}{\alpha e}\left((i_{pas} + i_{pin}P - \beta)\alpha + \ln\left(\frac{(P_{tot}-P)\mathrm{e}^{\alpha(-F_1+\beta)} + P_{tot} - 2P}{P}\right)\right) \tag{S.30}$$

This line is able to intersect three times with the auxin equilibrium line, thus bistability occurs at the membrane segment level (similar to **MS.III**, fig S.3**C**). Similar to the Smith et al. [2006] model, this PIN equilibrium line can shift to the right or left due to changes in the context of the cell and so lose its bistability.

Due to the finite PIN pool, that is at all times divided between P_0 and P_1, there is polarity at the single cell level (variant **SC.II**, fig S.4**B**).

S.5.1.6 Alim and Frey (2010)

Alim and Frey [2010] use the same assumptions as Feugier and Iwasa [2006] (in our analysis, disregarding the flux-bifurcator), i.e. the PIN pool is limiting and PIN exocytosis depends superlinearly on the flux (PIN equilibrium line Flux.2.b). Hence, the Alim and Frey [2010] model belongs to membrane segment variant **MS.III** and single cell variant **SC.II** (fig S.3**C** and S.4**B**).

S.5.2 Concentration based models

S.5.2.1 Jönsson *et al.* (2006)

The model constructed by Jönsson et al. [2006] is a concentration-based model used to simulate phyllotaxis. In this model auxin in the neighbouring cells feeds back on the PIN localisation at the membrane segments and membrane segments compete for a limiting PIN pool. Auxin transport is non-saturating. The authors apply two different feedback functions, a linear one and a superlinear, saturating one (where $k_{on} = \frac{A^3}{h^3+A^3}$). The linear feedback function is used for analysis on spacing of peaks. In this case, it is assumed that the PIN dynamics are in equilibrium and that all PINs recide on the membrane. Hence the PIN equilibrium line is given by:

$$P = \frac{P_{tot}A}{\sum_i^n A_i} \tag{S.31}$$

Additionally, when studying a 1D file, the authors assume that the pumping of auxin by PINs is linear. Therefore, the auxin equilibrium line is given by eq S.3. These equilibrium lines can only intersect once, hence the linear feedback does not allow for bistable behaviour at the membrane segment level (variant **MS.I**, fig S.3**A**). The superlinear, saturating feedback that is used for the 2-dimensional simulations, introduces non-linearity into the PIN equilibrium line and therefore does allow for bistable behaviour (variant **MS.III**, fig S.3**C**).

The linear feedback, combined with linear pumping, does not give cell polarity at the single cell level (variant **SC.I**, fig S.4**A**), whereas the superlinear, saturating feedback, combined with saturated pumping, does (variant **SC.II**, fig S.4**B**).

Interestingly, our tissue level analysis does show self-organised behaviour for the linear feedback function and linear pumping that does not give bistability or cell polarity. To further investigate this alternative Turing-like self-organising behaviour, we performed a bifurcation analysis on a 1-dimensional five cell model, consisting of 5 auxin and 10 PIN equations, specifically focusing on the parameter regions for which the cells in the tissue become polarised. Fig S.5 shows a bifurcation diagram of how the tissue level equilibria in a ring of five cells depend on the parameters P_{tot} and k_{off} for the Jönsson et al. [2006] model and a modified model that does not have a limiting PIN pool (eq Conc.3.a with $n = 1$). In order to obtain insight in whether polar equilibria occur, we introduce the variance (V) which reflects the difference in PIN levels on opposing membranes. Furthermore, to test for consistent polarisation among all 5 cells of the tissue, we sum these differences across cells. Thus, a large variance implies the presence of a strongly polar equilibrium in all cells of the tissue, whereas a variance of 0 implies that all cells are apolar. Variance is thus formally defined as:

$$V = \sum (P_{i,0} - P_{i,1})^2 \quad \text{with } i = 1, 2, 3, 4, 5 \tag{S.32}$$

For the Jönsson et al. [2006] model we see that, above a critical P_{tot} and below a critical k_{off} value, a bifurcation occurs that leads to a situation with persistenly polarised cells across the tissue. In contrast, no such behaviour was found for the alternative model without a limiting PIN pool. We therefore conclude that the limiting PIN pool is required to obtain the self-organising behaviour found in the Jönsson et al. [2006] model.

S.5.2.2 Merks *et al.* (2007)

In the concentration-based model by Merks et al. [2007], efflux of auxin through the PINs saturates. The authors do not take into account production and decay of auxin in all cells, but allow auxin to flux into the tissue from a source and to leave it through a sink. Again, we approximate this global production and decay with local, cellular production and decay processes. Therefore we can use equation S.2 for the auxin which provides the auxin equilibrium line in eq S.4.

In contrast to other models in which a limiting PIN pool is assumed, the authors describe the cytosolic PINs (P_c) dynamically:

$$\frac{dP_c}{dt} = p_{pin} - d_{pin}P_c + k_{off} \sum P_i - \sum \frac{k_{on}P_c}{k_m + P_c} \tag{S.33}$$

In which p_{pin} is the production of PINs, whereas d_{pin} is the decay rate. Endocytosis as well as exocytosis are summed over all membrane segments of the cell. The exocytosis rate saturates with the amount of PINs in the cytosol and the half-maximum rate is obtained when $P_c = k_m$.

At the membrane segment level, P is described as:

$$\frac{dP_i}{dt} = \frac{k_{on}P_c}{k_m + P_c} - k_{off}P_i \tag{S.34}$$

k_{on} depends on auxin in a saturating manner:

$$k_{on} = \frac{k_{on_f}A}{h_A + A} \tag{S.35}$$

Setting equation S.33 to 0, given only one membrane segment ($\sum P_i = P$) and assuming that PIN production and decay are in equilibrium gives us a measure for P_c. Filling this and k_{on} from equation S.35 into equation S.34

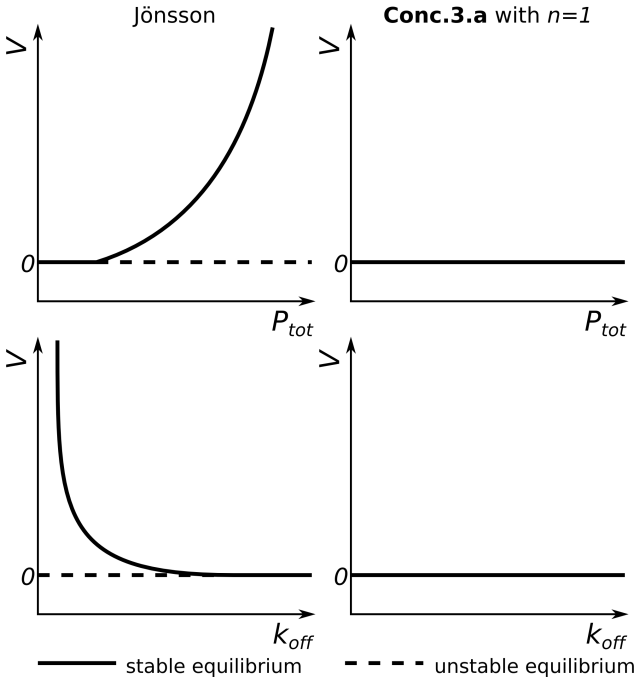

Figure S.5: Bifurcation diagrams for a ring of cells in the Jönsson et al. [2006] model and eq Conc.3.a with $n = 1$. Dependence of variance V on P_{tot} (upper panels) and k_{off} (lower panels). The Jönsson et al. [2006] model shows stable equilibria in which $V > 0$ and, thus, permanent tissue polarisation occurs. The model with eq Conc.3.a with $n = 1$ has only one equilibrium for $V = 0$. Hence, no polarity is found.

and setting the resulting $\frac{dP}{dt}$ equation to 0 provides the following PIN equilibrium line (similar to eq Flux.3.b) for P at the membrane segment:

$$P = \frac{p_{pin} k_{on_f} A}{k_{off}(p_{pin} A + d_{pin} k_m A + p_{pin} h_A + d_{pin} k_m h_A)} \tag{S.36}$$

This line can intersect thrice with the auxin equilibrium line (fig S.3**D**), therefore bistability can occur at the membrane segment level (variant **MS.IV**).

The single cell phase plane is shown in fig S.4**D**. In this model PIN concentrations change not only due to exo- and endocytosis, but also due to production and decay of PINs. It is noteworthy that decay of PINs occurs only for cytosolic but not for membrane bound PINs. As a result, although the cytosolic PIN pool has a fixed equilibrium size, the total amount of PINs that a cell contains is not fixed, but varies with the amount that is present on the membrane segments. As a consequence, the PIN pool in this model is effectively unlimiting, as can be seen from the additional bipolar equilibrium at the single cell level. Hence, the model falls into single cell category **SC.IV**.

S.5.2.3 Newell *et al.* (2007)

For their combined concentration- and physical force-based model, Newell et al. [2007] used the PIN and auxin equations first described by Jönsson et al. [2006] for the 1D cell file (linear feedback, linear auxin transport) and translated these into continuous equations. However, they did not study the model with a QSS assumption for the PIN cycling and did not assume that all the PINs reside on the membrane as done by Jönsson et al. [2006]. The auxin equilibrium line is given by eq S.3 and the PIN equilibrium line is given by eq Conc.1.b. As a result, the model is not bistable at the membrane segment level (variant **MS.I**, fig S.3**A**) and not polar at the single cell level (variant **SC.I**, fig S.4**A**). However, due to the limiting PIN pool and up-the-gradient PIN polarisation, this model is still able to self-organise at the tissue level, similar to the Jönsson et al. [2006] model with linear feedback and non-saturated auxin transport.

S.5.2.4 Sahlin *et al.* (2009)

Sahlin et al. [2009] developed a concentration-based model for phyllotaxis. They include apolar expression of AUX1, which cannot be included in our framework, because we do not explicitly model the cell wall. Auxin transport is saturated for high auxin concentrations, hence the auxin equilibrium line is given by eq S.4. The PIN pool is limiting, and several feedback functions have been used. The most simple feedback function is linear which, combined with the limiting PIN pool gives the PIN equilibrium line in eq Conc.1.b. Due to the combination of the non-linear auxin equilibrium line and the non-linear PIN equilibrium line, the model is bistable at the membrane segment level (variant **MS.IV**). At the single cell level, polarity occurs (variant **SC.II**).

S.5.3 Joined concentration- and flux-based model

Bayer et al. 2009 Bayer et al. [2009] incorporated both up-the-gradient and with-the-flux PIN polarisation into their model. Cells in the model apply one of these two mechanisms, deciding which one based on their auxin level. The auxin equation is the same as used in their previous model [Smith et al., 2006], which is described in the main text. The authors assume a limiting PIN pool at the single cell level and saturated transport of auxin (with co-operativity 2).

In the up-the-gradient feedback regime the model is identical to the [Smith et al., 2006] model. It thus falls into category **MS.III** at the membrane segment and shows bistable behaviour (fig S.3**C**). At the single cell level, the model is polar (variant **SC.II**, fig S.4**B**).

In the with-the-flux regime, the authors apply the same shape of feedback function, but substitute auxin concentration with a new variable "flux history" that depends on the net efflux (similar to eq Flux.3.b):

$$P = \frac{P_{tot} b^F}{\sum_n b^{F_i}} \tag{S.37}$$

in which b is a base parameter that the authors set to 2 or 3 and the sum is taken over the fluxes over all membrane segments. The resulting PIN equilibrium line has a superlinear saturating shape that can intersect three times with the auxin equilibrium line given by eq S.4 (variant **MS.III**, fig S.3**C**). Hence, also in the with the flux regime, the model supports membrane bistability, and cell polarity (variant **SC.II**, fig S.4**B**).

P_{tot} is calculated dynamically, as in the model by [Smith et al., 2006], however, since all the PINs are assumed to be on the membrane, these models do not have the issue described for the model by Merks et al. [2007], namely that the PIN pool is effectively unlimited.

S.5.4 Mechanistic models

Heisler et al. 2010 In the model by Heisler et al. [2010], PIN localisation is determined by wall stress which in turn is dependent on auxin concentrations within neighbouring cells. Active transport of auxin is saturated, therefore the auxin dynamics are determined by equation S.2 and the corresponding auxin equilibrium line is given by equation S.4. As in their previous model [Jönsson et al., 2006], the authors assume that PIN dynamics are at all times in equilibrium and that all PINs reside on the membrane. They write the following dependency of PINs on the membrane stresses experienced by a membrane segment:

$$P = \frac{P_{tot} k_2 s^n}{1 + \sum k_2 s_i^n} \tag{S.38}$$

in which P_{tot} is the total amount of PINs in a cell, s is the stress experienced by a single membrane segment, k_2 is the level by which PINs depend on the stress and n is the co-operativity with which this happens. The sum is taken over all the membrane segments belonging to one cell. For a single membrane segment, we can write:

$$P = \frac{P_{tot} k_2 s^n}{1 + k_2 s^n + k_2 h^n} \tag{S.39}$$

In which h represents the stresses experiences by the other membrane segments that are not in focus and thus assumed to be constant. The stress negatively depends on wall elasticity as follows:

$$s = \frac{F}{A_0(1 + \frac{E(A)}{E(A_i)})} \tag{S.40}$$

F is the isotropic force on each wall, A_0 is the cross section of a cell and A_i is the auxin content of the cell to which the membrane segments belongs and is thus assumed to be constant. $E(A)$ is the wall elasticity which is a function of auxin in the neighbouring cell:

$$E = E_{min} + \frac{(E_{max} - E_{min}) k_3^m}{A + k_3^m} \tag{S.41}$$

E_{min} is the minimal and E_{max} the maximal wall elasticity. E decreases with auxin. k_3 is a saturation constant and m is the co-operativity with which elasticity depends on auxin. The full PIN equilibrium line is obtained by substituting S.40 and S.41 into S.39 Because of its length and complexity we refrain from giving it explicitly. However, for the parameters used by the authors, it can be shown to describe a sublinear, saturating, function (similar to eq Conc.3.a). However, considering that the auxin equilibrium line is also a non-linear line, this should theoretically allow for three intersection points between the equilibrium lines and thus the model falls into membrane segment category **MS.IV** (fig S.3**D**). In line with this and because of the limiting PIN pool, we expect polarity at the single cell level (variant **SC.II**, fig S.4**B**).

Wabnik et al. 2010 Wabnik et al. [2010] developed a PAT model in which auxin in the cell wall, by binding to a receptor, inhibits endocytosis of PINs from the nearest membrane. In order to study this model, we extended our framework to include the cell wall. In our membrane segment model, A is the concentration of auxin in the neighbouring cell. For this model, we use A for the concentration of auxin in the cell wall adjoining the membrane segment of interest. The dynamics are the same, the cell wall receives auxin by active and passive transport over

the membrane segment of interest and it loses auxin by influx. Hence, we can use the same equation that we used for auxin in the neighbouring cells for saturated efflux (equation S.2 and corresponding equilibrium line S.4).

Similar to Merks et al. [2007], the authors model the cellular PIN pool dynamically, in this case, however, feedback is implemented through the endocytosis rate k_{off}. The cytosolic PIN pool is given by:

$$\frac{dP_c}{dt} = p_{pin} - d_{pin}P_c + \sum_n k_{pin}P_i - \sum_n k_{on}P_c \tag{S.42}$$

In which the sums are taken over all membrane segments belonging to one cell.

The equation for PINs on the membrane segment is:

$$\frac{dP}{dt} = k_{on}P_c - k_{off}P \tag{S.43}$$

For the formation of complexes (C) between auxin and receptor in the cell wall, we use, as in the original publication, a QSS assumption. Thus allows us to write

$$C = \frac{2r_T A}{2k_d + \sum_n A_i} \tag{S.44}$$

In which r_T is the total amount of receptors in the cell wall, k_d is a saturation constant and the sum is taken over all segments of the cell wall.

For the membrane segment level, since we assume auxin concentrations to be constant in all compartments other than the cell wall segment of interest, we can rewrite eq S.44 as:

$$C = \frac{2r_T A}{2k_d + h + A} \tag{S.45}$$

In which h now represents the auxin concentrations in other cell wall compartments. The endocytosis rate of PINs now depends on the amount of complex as such:

$$k_{off} = k_{off_b} + \frac{k_{off_f}}{1 + C} \tag{S.46}$$

The PIN equilibrium line that is obtained by substituting equation S.46 and S.45 into S.43 is a saturating, sublinear function. Hence, it can intersect more than once with the non-linear auxin equilibrium line and there is bistability at the membrane segment level (variant **MS.IV**, fig S.3**A**).

For the single cell level, as in Merks et al. [2007], the PIN pool in the Wabnik et al. [2010] model increases with the amount of PINs that are on the membrane. Therefore, it is effectively unlimiting. There is, however, still a slight effect of P_0 on P_1 and *vice versa*, therefore the PIN equilibrium lines are not completely horizontal and vertical and the model belongs to category **SC.IV**.

To study the tissue behaviour, we extended the framework to include cell walls. We found that the model is able to self-organise after a perturbation is provided to one of the cells. The resulting PIN polarisation is similar to with-the-flux models, where the PINs point from the source to the sink in a cell file, and all point in the same direction in a ring of cells. In order to obtain this behaviour, auxin diffusion in the cell wall must be sufficiently low, to allow for the formation of an auxin gradient. Therefore, it appears that the model's self-organising behaviour relies on across-cell wall polarity as well as cell polarity.

References

K Alim and E Frey. Quantitative predictions on auxin-induced polar distribution of PIN proteins during vein formation in leaves. *The European Physical Journal E*, 33:165–173, 2010.

EM Bayer, RS Smith, T Mandel, N Nakayama, M Sauer, P Prusinkiewicz, and C Kuhlemeier. Integration of transport-based models for phyllotaxis and midvein formation. *Genes and Development*, 23(3):373–384, 2009.

FG Feugier and Y Iwasa. How canalization can make loops: A new model of reticulated leaf vascular pattern formation. *Journal of Theoretical Biology*, 243(2):235–244, 2006.

FG Feugier, A Mochizuki, and Y Iwasa. Self-organization of the vascular system in plant leaves: Inter-dependent dynamics of auxin flux and carrier proteins. *Journal of Theoretical Biology*, 236(4):366–375, 2005.

H Fujita and A Mochizuki. Pattern formation of leaf veins by the positive feedback regulation between auxin flow and auxin efflux carrier. *Journal of Theoretical Biology*, 241:541–551, 2006.

MG Heisler, O Hamant, P Krupinski, M Uyttewaal, C Ohno, H Jönsson, J Traas, and EM Meyerowitz. Alignment between PIN1 polarity and microtubule orientation in the shoot apical meristem reveals a tight coupling between morphogenesis and auxin transport. *PLoS Biology*, 8(10), 2010.

H Jönsson, MG Heisler, BE Shapiro, EM Meyerowitz, and E Mjolsness. An auxin-driven polarized transport model for phyllotaxis. *Proceedings of the National Academy of Sciences of the United States of America*, 103(5): 1633–1638, 2006.

RMH Merks, Y Van de Peer, D Inzé, and GTS Beemster. Canalization without flux sensors: a traveling-wave hypothesis. *Trends in Plant Science*, 12(94):384–390, 2007.

GJ Mitchison. A model for vein formation in higher plants. *Proceedings of the Royal Society of London - Biological Sciences*, 207(1166):79–109, 1980.

GJ Mitchison. The polar transport of auxin and vein patterns in plants. *Phil. Trans. R. Soc. Lond.*, 295:461–471, 1981.

AC Newell, PD Shipman, and Z Sun. Phyllotaxis: cooperation and competition between mechanical and biochemical processes. *Journal of Theoretical Biology*, 251:421–439, 2007.

P Sahlin, B Söderberg, and H Jönsson. Regulated transport as a mechanism for pattern generation: Capabilities for phyllotaxis and beyond. *Journal of Theoretical Biology*, 258(1):60–70, 2009.

RS Smith, S Guyomarc'h, T Mandel, D Reinhardt, C Kuhlemeier, and P Prusinkiewicz. A plausible model of phyllotaxis. *Proceedings of the National Academy of Sciences of the United States of America*, 103(5):1301–1306, 2006.

K Wabnik, J Kleine-Vehn, J Balla, M Sauer, S Naramoto, V Reinöhl, RM Merks, W Govaerts, and J Friml. Emergence of tissue polarization from synergy of intracellular and extracellular auxin signaling. *Molecular Systems Biology*, 6(447), 2010.